5-DOF Magnetic Levitation Control of a Steel Plate Using Observation of the Supported Weight

No. 84

Ryuta, Sasaki & Susumu, Torii

Department of Electrical and Electronic Engineering, Musashi Institute of Technology, Tokyo, Japan

ABSTRACT: The magnetic levitation of steel-plate have been studied for the purpose of non-contact conveyance. Most of the systems which are dealt within these studies consist of electromagnets, gap sensors and a controller. This kind of system in general has no guide force. Therefore, as soon as a lateral external force acts, the component force of gravity easily makes a steel-plate sideslip. This paper proposes to estimate and control the horizontal displacement of a steel-plate that moves from the equilibrium position by using observation of the electromagnetic force.

1 INTRODUCTION

In recent years, the demand for high-value added steel plates as typified by automotive steels has been increasing. They are conveyed with rollers in manufacturing process. However, the process hurt their surface for contact friction with rollers. The non-contact conveyance method of steel-plates using electromagnetic suspension (EMS) has been studied as one of the solutions to avoid the problem. This system in general is stabilized in three degrees of freedom (translation in a direction plus rotation in two directions) by feedback control using gap sensors. However, there is not any force which provides static stability or dynamic stability in both lateral and longitudinal directions. As soon as a horizontal force acts, the component force of gravity easily makes a steel-plate sideslip. This phenomenon is one of the main causes that prevent the technology from the practical application.

Some attempts to avoid a sideslip have been studied. Nakagawa has suggested a effective method for correcting levelness of a steel-plate with positioning sensors (Nakagawa 2000). Oshinoya et al. have made many active studies for horizontal non-contact positioning with lateral-directional flux (Oshinoya et al. 2002). Most previous studies use the displacement sensors for sensing sideslip.

Differently from these approaches, we have proposed to control the sideslip of a steel-plate by using observation of the electromagnetic forces. When a levitated steel-plate has horizontal displacement, each electromagnetic force fluctuates in response to the displacement. We use load cells for the purpose of sensing the electromagnet force. In addition, we also use general displacement sensors to detect each gap length between an electromagnet and a supported point. By calculating the obtained values, the motion of a steel-plate is observed in the five degrees of freedom except yaw. Therefore, we can design the maglev control system with the use of optimal control in five d.o.f.s .

In this paper, first we show the modeling of the controlled object and designing the maglev control system. Next, the simulation results are described for evaluating the effectiveness and adequacy of the proposed method. Finally, we discuss the problems for the implementation of the control system.

2 CONTROLLED OBJECT

2.1 The Observation of Motion

Figure 1 depicts the conceptual diagram of four-point support system using EMS. In order to exclude the problems caused by flexure, we assume that a

levitated steel-plate is not a thin steel plate but a rigid body. An unrestrained steel-plate has three translational d.o.f.s and three rotational d.o.f.s, a total of six d.o.f.s.

To simplify the discussion, this paper mainly deals with the dynamics model of two dimensional rigid body described in Figure 2. In the two dimensional model, a steel-plate have three d.o.f.s. – pitch, vertical translation and lateral translation. Figure 3 illustrates the three modes of motion (Yamamura 1979). The vertical displacement of the center of gravity from the equilibrium position is shown in Equation 1. The pitch angle is shown in Equation 2:

$$z'_G = z'_2 + \left(\frac{1}{2} - \frac{x'}{D}\right)(z'_1 - z'_2), (1)$$

$$\theta = \theta' = \tan^{-1}\left(\frac{z_1 - z_2}{D}\right) \approx \frac{z'_1 - z'_2}{D}, (2)$$

where:
z'_G = the vertical displacement of the center of gravity from the equilibrium position;
z_1, z_2 = the gap length between a supported point and an electromagnet;
z'_1, z'_2 = the deviation of each gap length from the equilibrium position;
$\theta = \theta'$ = the pitch angle;
$x = x'$ = the sideslip displacement, or the horizontal displacement of the center of gravity from the equilibrium position;
and D = the distance between the electromagnets.

The sideslip displacement x is unobservable by gap sensors. We therefore use load cells as force sensors in order to estimate x from the measured electromagnetic forces. The equation for calculating x is expressed as follows:

$$x' = x = D\left(\frac{1}{2} - \frac{m_1 g}{M_G g}\right), \quad (3)$$

$$\frac{T}{2} < D < T, \quad -\frac{T-D}{2} < x' < \frac{T-D}{2}, (4)$$

where:
M_G = the mass of a steel-plate;
$m_1 g, m_2 g$ = the weight at each supported point;
and T = the length of a steel-plate.

From the Eq. 3, we can plot the change of supported weight with respect to sideslip displacement on Figure 4. In Fig. 4, $m_1 g$ and $m_2 g$ are linearly-varying with respect to x. Therefore, the sideslip displacement can be determined uniquely by the measured values of $m_1 g$ and $m_2 g$.

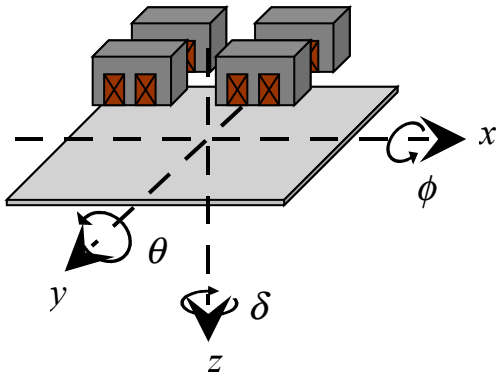

Figure 1. Conceptual diagram of four-point support system using EMS

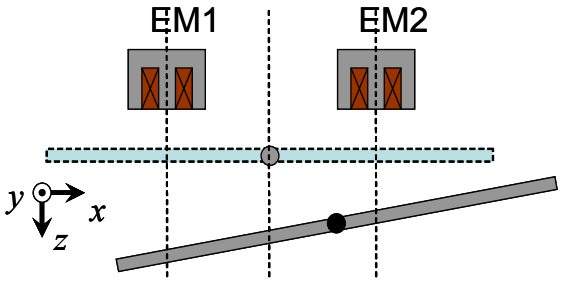

Figure 2. Two dimensional dynamic model with three d.o.f.s

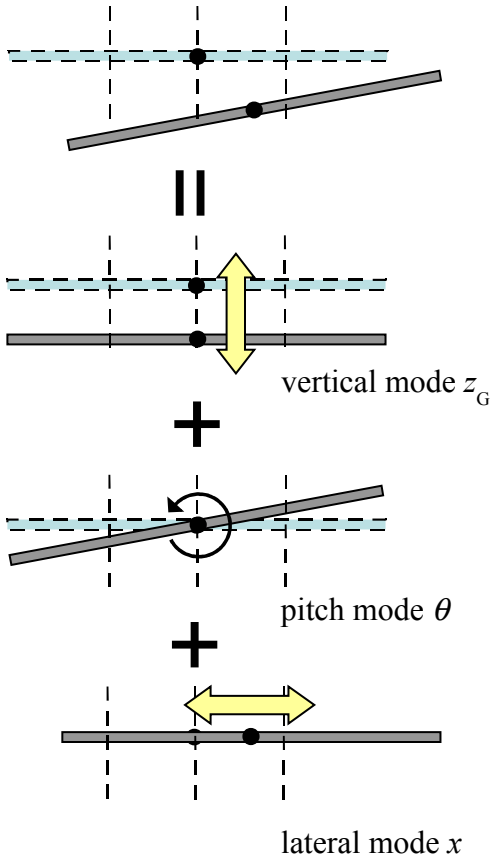

Figure 3. Three modes of rigid steel-plate motion

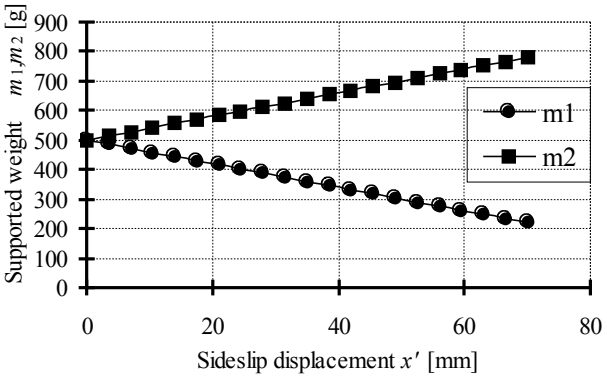

Figure 4. Supported weights (m_1,m_2) versus sideslip displacement (x) (M_G=1kg, T=400mm, D=250mm)

2.2 Modeling

In the vertical mode, the equation of motion of steel-plate in the vertical direction is expressed as follows:

$$M_G \ddot{z}_G = M_G g - (f_{G1} + f_{G2}), \quad (5)$$

$$f_{G1} = \frac{k_1 {i_{G1}}^2}{(Z_{k1} + z_G)^2}, \quad f_{G2} = \frac{k_2 {i_{G2}}^2}{(Z_{k2} + z_G)^2}, \quad (6)$$

where:
f_{G1},f_{G2} = the electromagnetic forces in the vertical mode;
i_{G1},i_{G2} = the exciting currents in the vertical mode;
and k_j,Z_{kj} = the specific constants of electromagnet.

If there is not any external force other than gravity and electromagnetic forces, the steel-plate is displaced laterally only by the component force of gravity with pitch motion. Therefore, it is impossible to write the equation of motion only in lateral mode. We need to discuss the coupled mode of the both lateral and pitch motion. In the coupled mode, the equation of motion of steel-plate in the direction of pitch is expressed as follows:

$$J_\theta \ddot{\theta} = -r_1 f_{\theta x1} + r_2 f_{\theta x2} = -\left(\frac{D}{2} + x\right)\frac{k_1 {i_{\theta x1}}^2}{(Z_{k1} + z_{\theta x1})^2} + \left(\frac{D}{2} - x\right)\frac{k_2 {i_{\theta x2}}^2}{(Z_{k2} + z_{\theta x2})^2}, \quad (7)$$

$$z_{\theta xj} = Z_0 + (-1)^j \frac{z_2 - z_1}{2} + x \tan\theta, \quad (8)$$

where:
J_θ = the moment of inertia of a steel-plate;
r_j = the perpendicular distance of a supported point to the center axis which pass through the center of gravity;
ρ = the linear density of a steel-plate;
$f_{\theta xj}$ = the electromagnetic force in the coupled mode of pitch and lateral motion;
$i_{\theta xj}$ = the exciting current in the coupled mode;
$z_{\theta xj}$ = the gap length between a supported point and an electromagnet in the coupled mode;
and j = the number of electromagnet.

In the same mode, the equation of motion of steel-plate in the lateral direction is expressed as follows:

$$M_G \ddot{x} = -(M_G g \sin\theta)\cos\theta. \quad (9)$$

The linearizations of the above nonlinear differential equations at an equilibrium point are expressed as follows:

$$\left.\begin{aligned} M_G \ddot{z}'_G &= \alpha_G z'_G - (\beta_{G1} i'_{G1} + \beta_{G2} i'_{G2}) \\ \alpha_G &= \sum_{j=1}^{2} \frac{2k_j {I_{0j}}^2}{(Z_{kj} + Z_0)^3}, \quad \beta_{Gj} = \frac{2k_j I_{0j}}{(Z_{kj} + Z_0)^2}, \quad (j = 1,2) \end{aligned}\right\}, \quad (10)$$

$$\left.\begin{aligned} J_\theta \ddot{\theta}' &= \alpha_\theta \theta' - \gamma_\theta x' - \beta_{\theta 1} i'_{\theta x1} + \beta_{\theta 2} i'_{\theta x2} \\ \alpha_\theta &= \frac{D^2}{4}\alpha_G,\ \beta_{\theta j} = \frac{D}{2}\beta_{Gj},\ \gamma_\theta = \sum_{j=1}^{2} \frac{k_j {I_{0j}}^2}{(Z_{kj} + Z_0)^2} \end{aligned}\right\}, \quad (11)$$

$$M_G \ddot{x}' = -M_G g \theta', \quad (12)$$

where:
Z_0 = the equilibrium gap length (or gap command);

I_{0j} = the equilibrium currents (or current commands);
i'_{Gj} = feedback input currents in vertical mode; and $i'_{\theta xj}$ = feedback input currents in the coupled mode of pitch and lateral motion.

2.3 State Equations

Given the above linear differential equations, we can apply state feedback to stabilize the maglev system. The state equations of controlled objective are expressed as follows:

$$\dot{\boldsymbol{x}} = A\boldsymbol{x} + B\boldsymbol{u}, \quad (13)$$

$$\boldsymbol{x} = \begin{bmatrix} z'_G \\ \dot{z}'_G \end{bmatrix},\ \boldsymbol{u} = \begin{bmatrix} i'_{G1} \\ i'_{G2} \end{bmatrix},$$
$$A = \begin{bmatrix} 0 & 1 \\ \dfrac{\alpha_G}{M_G} & 0 \end{bmatrix},\ B = \begin{bmatrix} 0 & 0 \\ -\dfrac{\beta_{G1}}{M_G} & -\dfrac{\beta_{G2}}{M_G} \end{bmatrix}, \quad (14)$$

$$\left.\begin{aligned} \boldsymbol{x} &= \begin{bmatrix} \theta' \\ \dot{\theta}' \\ x' \\ \dot{x}' \end{bmatrix},\ A = \begin{bmatrix} 0 & 1 & 0 & 0 \\ \dfrac{\alpha_\theta}{J_\theta} & 0 & -\dfrac{\gamma_\theta}{J_\theta} & 0 \\ 0 & 0 & 0 & 1 \\ -g & 0 & 0 & 0 \end{bmatrix} \\ \boldsymbol{u} &= \begin{bmatrix} i'_{G1} \\ i'_{G2} \end{bmatrix},\ B = \begin{bmatrix} 0 & -\dfrac{\beta_{\theta 1}}{J_\theta} & 0 & 0 \\ 0 & \dfrac{\beta_{\theta 2}}{J_\theta} & 0 & 0 \end{bmatrix} \end{aligned}\right\}. \quad (15)$$

Since the matrix ***A*** in Eq. 15 is not block diagonal matrix, it's instantly noticeable that pitching and lateral motion are not independent of each other.

3 EVALUATION BY SIMULATION

3.1 Simulation Model and Conditions

We studied effectiveness and adequacy of the proposed system by computer simulation. Figure 5 shows a nonlinear block diagram about the individual electromagnet system. Figure 6 shows the simplified block diagram of the entire control system. The simulation conditions and the state feedback gains designed with LQR are given in Table 1 and Table 2 respectively. Gain K_A and Gain K_B were designed for the purposes of comparison between them in such a way that the latter weighting factors on the lateral displacement term and lateral velocity term are larger than the former ones.

In order to discuss the performance of lateral control, we would like to simulate the responses to external force act in lateral direction. The disturbances to induce a sideslip include an external impulsive force, the eccentric load of a steel-plate and the installation error of electromagnets. We thereby give the following conditions.

- External impulsive force (0.04 Ns, 4 ms, 10 N) in the lateral direction
- Step load disturbance (100 g) at the point supported by electromagnet-2
- Installation error of electromagnets (given by installing electromagnet-1 just 1.0 mm higher than electromagnet-2)

In all simulation, we used the nonlinear simulation model in order to evaluate the proposed system as close to true system as possible.

3.2 Simulation Results and Discussing

Figure 7 shows the simulation results of the impulse disturbance responses. In this figure, any state quantities converge to the equilibrium values in about three to four seconds. The response of the sideslip with K_B converges about 0.5 seconds faster than with K_A. Moreover, the amplitude of the sideslip with K_B is about 7.5 millimeters smaller than with K_A. In contrast, as in figures of the other state quantities and the exciting current, each amplitude with K_B is larger than with K_A. It is by reason that larger pitch angle is needed for faster lateral control because of cause-and-effect relationship shown in Eq. 12. Therefore, the performance of response depend on the acceptable pitch angle. However, it is hard to make the response faster because of the gap length of only a few millimeters.

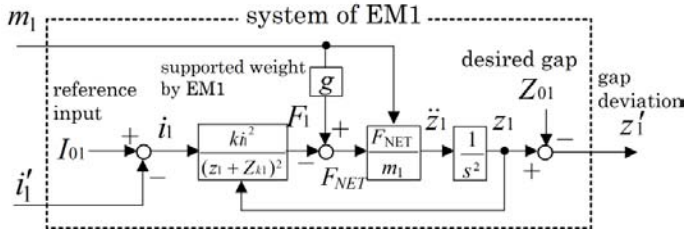

Figure 5. Block diagram about the individual electromagnet system

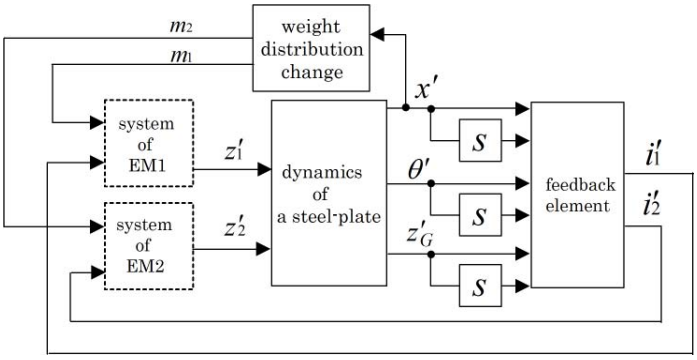

Figure 6. Entire two-point support control system

Table 1. Simulation conditions

Constant	unit	value
Length of steel-plate T	mm	450
Thickness of steel-plate	mm	1.0
Mass of steel-plate M_G	kg	0.53
Moment of inertia of steel-plate J_θ	kgm^2	0.004
Distance between electromagnets D	mm	330
Gap command Z_0	mm	3.0
Current command I_0	A	1.06
Cross sectional area of magnet core (E-core)	mm^2	175
Number of turns in a winding	turns	580
Self-inductance L	mH	24.7
Electromagnetic constant k		3.7E-5
Electromagnetic constant Z_k		0.001

Table 2. State feedback gains

State variable	K_A		K_B	
	EM1	EM2	EM1	EM2
z'_G	-530			
dz'_G/dt	-7.63			
θ'	-92.1	92.1	-94.1	94.1
$d\theta'/dt$	-2.34	2.34	-2.34	2.34
x'	11.0	-11.0	16.8	-16.8
dx'/dt	9.38	-9.38	13.6	-13.6

Note that the gap z_2 closes to zero at peak point of undershoot. The peak value with K_B is 0.2 millimeters as against 1.0 millimeter for K_A. In case of K_B, if a little larger external force acts, the steel-plate is expected to come in contact with the electromagnet (this means $z_2 \leq 0$). Thus, there are trade-off between the limit of external force and the response of sideslip.

Figure 8 shows the simulation results of the step disturbance responses. While there is a certain level of steady-state error, the sideslip converges to the steady state without noticeable oscillation. These results indicate that the system have robustness to disturbances and errors such as the installation error of devices, the uncertainty of controlled object, and the parameter change including coil resistance and inductance.

4 THE PROBLEMS FOR IMPLEMENTATION

4.1 The Problem of Observation

In the experiment apparatus, the load cells are installed between the exterior frame and each electromagnet. They observe the reaction forces which act on each electromagnet. Thus the observed values are not the weight of a levitated steel-plate but the levitation force. The equation of motion of the steel-plate at any supported point is expressed as follows:

$$m_j \ddot{z}_j = m_j g - f_j . \quad (16)$$

As is clear from Eq. 16, the observed value f_j equals to the weight $m_j g$ only when the steel-plate is static in vertical direction. In case that the steel-plate has acceleration in the vertical direction, we can not observe sideslip motion because the calculating formula of x is shown in Eq. 3. Therefore, it is necessary to use the following formula given by substituting Eq. 16 into Eq. 3:

$$x = (-1)^j \frac{D}{M_G} \frac{f_j}{(\ddot{z}_j - g)} . \quad (17)$$

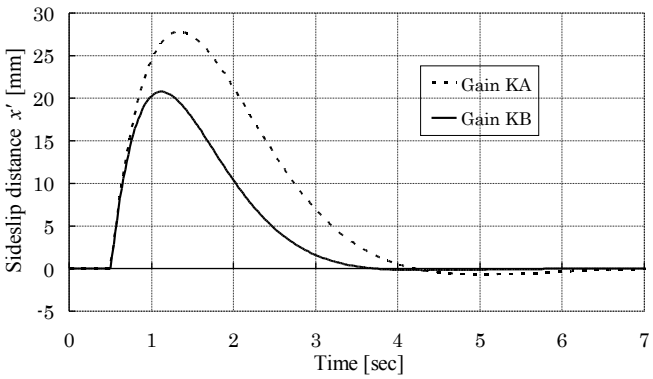

(a) Sideslip displacement (lateral displacement) x

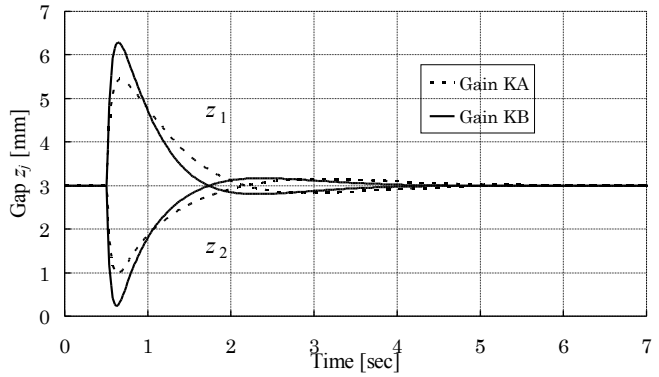

(b) Gap length z_j

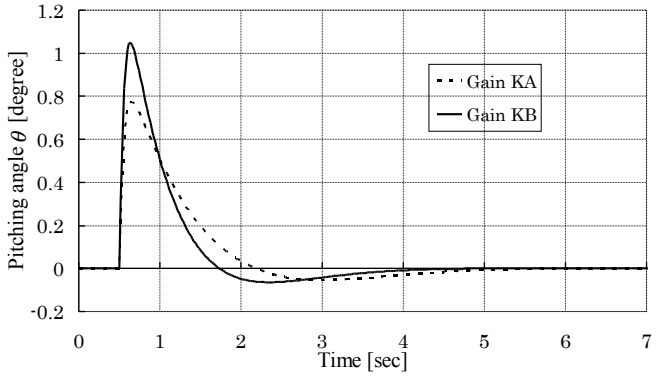

(c) Pitching angle θ

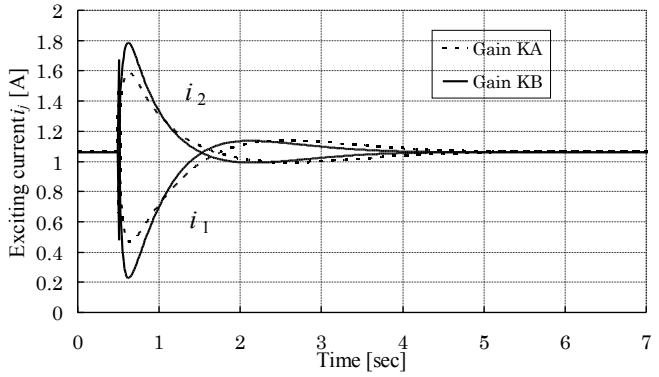

(d) Exciting current i_j

Figure 7. Simulation results of the impulse disturbance (0.04Ns, 4ms, 10N) responses with two dimensional nonlinear model

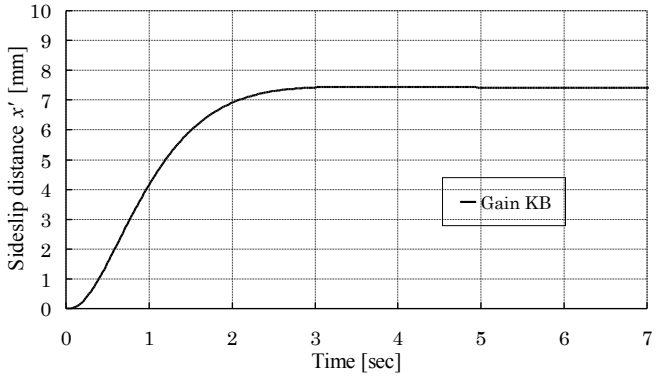

(a) Response of sideslip to step load disturbance (100g) at the point supported by electromagnet-2

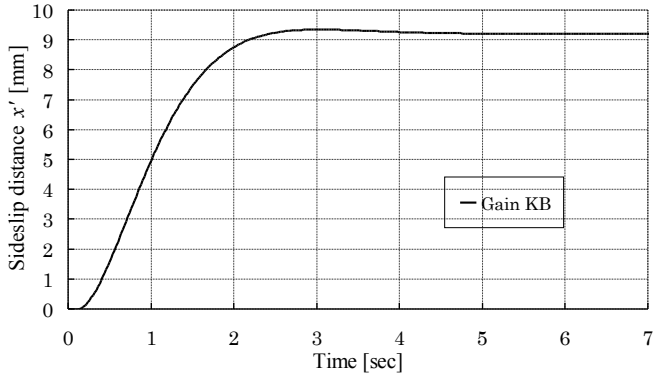

(b) Response of sideslip to the installation error of electromagnets (given by installing electromagnet-1 just 1.0 mm higher than electromagnet-2)

Figure 8. Simulation results of the step disturbance responses with two dimensional nonlinear model

From Eq. 17, acceleration value is needed for the observation of sideslip. We have no way of directly-detecting the acceleration. Therefore we use the second difference of detected gap length.

4.2 Improving Accuracy of Observation

The accurate measurement of electromagnetic force is an integral part of the sideslip control. However, since the output voltage of a load cell is low, the signal is susceptible to noise especially in measurement of a very small load. Some of the general noise-reduction includes shielding, a use of filters and separating noise sources.

In addition, other problem occurs in digital signal processing. Figure 9 shows the response of electromagnetic forces under the same conditions as Fig. 7. We can find that the change of the electromagnetic forces is rapidly. In particular, the pulse width (measured at 50 % of full height) is about 4.5 milliseconds. Therefore, high sampling rate is required for the measurement. The easiest solution meets the requirement is to use a sensor-interface which appears to answer our purpose, high enough sampling rate. We can, however, also discuss an alternative solution which slows the rate of change of electromagnetic force.

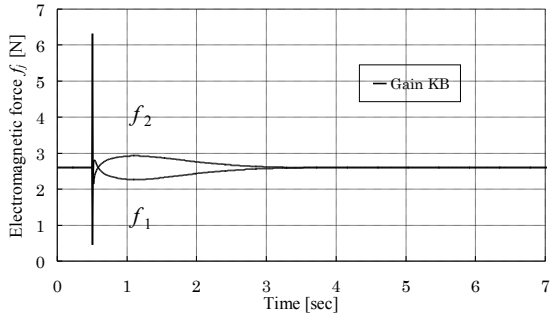

(a) Electromagnetic force f_j

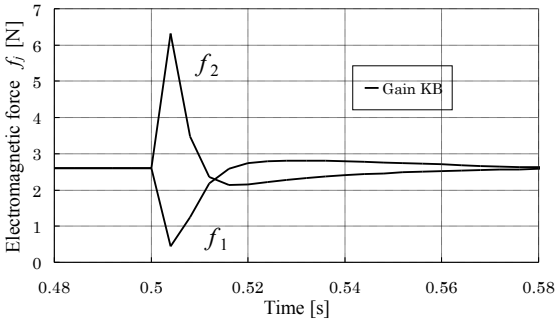

(b) Enlarged view f_j

Figure 9. Rapid change of electromagnetic force

4.3 Voltage Drive Control System

We discuss a voltage drive control as one of solutions which slow the response of electromagnets. By replacing input current signal by voltage signal, we can get the exciting current which lags applied voltage in the inductance of the electromagnetic coil. As a result, the responses of electromagnets are expected to be slowing. The state equations of the voltage drive system are expressed as follows:

$$\dot{\boldsymbol{x}} = A\boldsymbol{x} + B\boldsymbol{u}\,, (18)$$

$$\left.\begin{aligned} \boldsymbol{x} &= \begin{bmatrix} z'_G \\ \dot{z}'_G \\ i'_{G1} \\ i'_{G2} \end{bmatrix}, \quad A = \begin{bmatrix} 0 & 1 & 0 & 0 \\ \dfrac{\alpha_G}{M_G} & 0 & -\dfrac{\beta_{G1}}{M_G} & -\dfrac{\beta_{G2}}{M_G} \\ 0 & 0 & -R_1/L_1 & 0 \\ 0 & 0 & 0 & R_2/L_2 \end{bmatrix} \\ \boldsymbol{u} &= \begin{bmatrix} e'_{G1} \\ e'_{G2} \end{bmatrix}, \quad B = \begin{bmatrix} 0 & 0 & 1/L_1 & 0 \\ 0 & 0 & 0 & 1/L_2 \end{bmatrix}^T \end{aligned}\right\}, (19)$$

$$\left.\begin{aligned} \boldsymbol{x} &= \begin{bmatrix} \theta' \\ \dot{\theta}' \\ x' \\ \dot{x}' \\ i'_{\theta x1} \\ i'_{\theta x2} \end{bmatrix}, \quad A = \begin{bmatrix} 0 & 1 & 0 & 0 & 0 & 0 \\ \dfrac{\alpha_\theta}{J_\theta} & 0 & -\dfrac{\gamma_\theta}{J_\theta} & 0 & -\dfrac{\beta_{\theta 1}}{J_\theta} & \dfrac{\beta_{\theta 1}}{J_\theta} \\ 0 & 0 & 0 & 1 & 0 & 0 \\ -g & 0 & 0 & 0 & 0 & 0 \\ 0 & 0 & 0 & 0 & -R_1/L_1 & 0 \\ 0 & 0 & 0 & 0 & 0 & -R_2/L_2 \end{bmatrix} \\ \boldsymbol{u} &= \begin{bmatrix} e'_{\theta x1} \\ e'_{\theta x2} \end{bmatrix}, \quad B = \begin{bmatrix} 0 & 0 & 0 & 0 & 1/L_1 & 0 \\ 0 & 0 & 0 & 0 & 0 & 1/L_2 \end{bmatrix}^T \end{aligned}\right\}$$

, (20)

where:
e'_{Gj} = feedback input voltages in vertical mode;
$e'_{\theta xj}$ = feedback input voltages in the coupled mode of pitch and lateral motion;
L_j = the coil inductance;
and R_j = the coil resistance.

Note that each state vector includes the current deviations of each mode of motion. They are the virtual physical values. We therefore can not know the values singly by the actual measurement. Considering the equivalent circuit of each electromagnet as the independent system, we are able to make the full-order observer to estimate the currents. The state equation of the electric system of each electromagnet is expressed as follows:

$$\left.\begin{aligned} &\dot{\boldsymbol{x}} = A_{EM}\boldsymbol{x} + B_{EM}\boldsymbol{u}, \ \boldsymbol{y} = C_{EM}\boldsymbol{x} \\ &\boldsymbol{x} = \begin{bmatrix} i'_{Gj} & i'_{\theta xj} \end{bmatrix}^T, \ A_{EM} = \mathrm{diag}\begin{bmatrix} -R_j/L_j & -R_j/L_j \end{bmatrix} \\ &\boldsymbol{u} = \begin{bmatrix} e'_{Gj} & e'_{\theta xj} \end{bmatrix}^T, \ B_{EM} = \mathrm{diag}\begin{bmatrix} 1/L_j & 1/L_j \end{bmatrix}, \ C_{EM} = \begin{bmatrix} 1 & 1 \end{bmatrix} \end{aligned}\right\}$$

. (21)

Figure 10 shows the block diagram about the individual electromagnet of the voltage drive control system without the observers. Figure 11 shows an electric system of each electromagnet with the observer.

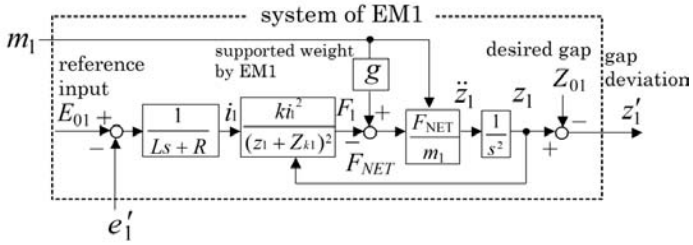

Figure 10. Block diagram about the individual electromagnet of the voltage drive control system

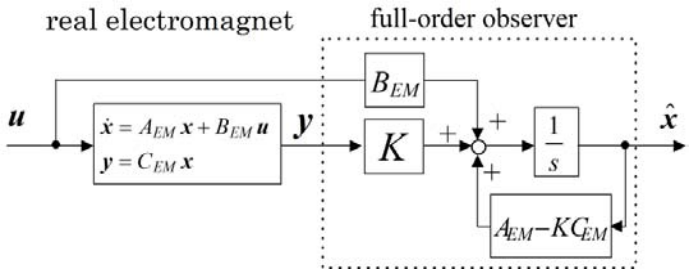

Figure 11. Electric system of each electromagnet with the full-order observer

Figure 12 shows the simulation results of impulse disturbance responses under the same conditions as the current drive, except for the reference input. The sideslip converges to the equilibrium position with a slight swing, though the response and stability are inferior as compared with the current drive. The pulse width is about 9.0 milliseconds. It is about twice as slow as that of current drive. Therefore, in the experiment done at the same sampling rate, the voltage drive system makes the transient changes of electromagnetic force observable with better accuracy than the current drive system.

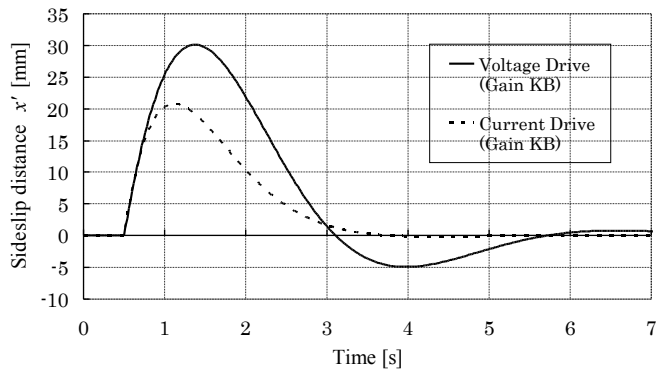

(a) Sideslip displacement (lateral displacement) x

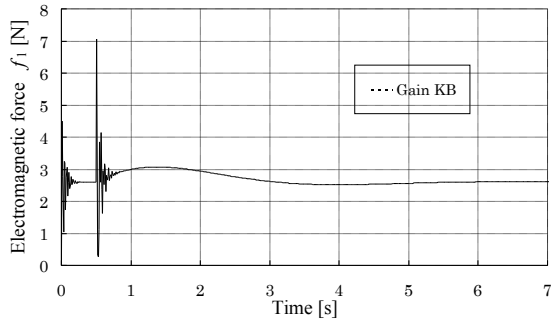

(b) Electromagnetic force f_1

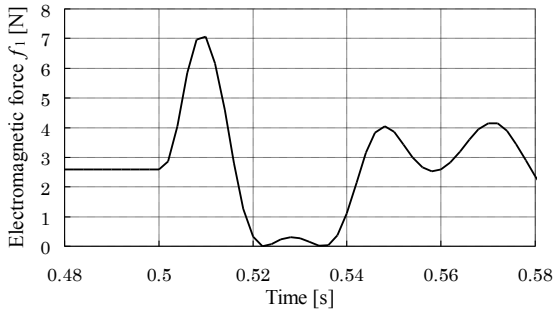

(c) Enlarged view f_1

Figure 12. Simulation results of impulse disturbance responses of voltage drive control system with two dimensional nonlinear model (reference voltage input E_0=6.0V)

5 CONCLUSIONS

This study aims to stabilize the EMS system both statically and dynamically in five d.o.f.s including lateral direction. As one of the methods, this paper described the EMS control method using observation of the electromagnetic force. The main conclusions are summarized as follows:

- The simulation results with the two dimensional model indicate the dynamic and static stability of the system.
- Due to the restriction of gap margin, the system sacrifices the response of lateral control to some extent.
- There are trade-off between the limit of external impulsive force and the response of lateral control.
- The system has robustness to model uncertainty.
- When a steel-plate is dynamic in vertical direction, the observation of sideslip need the estimate value of vertical acceleration.
- As compared with the current drive system, the voltage drive system has an advantage in the observation of sideslip, although it has a disadvantage in the response and stability.

The results obtained by simulation show the adequacy of the proposed system. Further studies with experimental support are necessary.

6 REFERENCES

T. Nakagawa, M. Hama, 2000 "*Study of Magnetic Levitation Control by Means of Correcting Gap Length Command for a Thin Steel Plate.*" The Institute of Electrical Engineers of Japan, Vol.120-D, No.4:pp.489-494

S. Hasegawa, Y. Oshinoya, K. Ishibashi, 2002 "*Improvement of Horizontal Noncontact Positioning Control for a Magnetic Levitation Steel Plate*." the Japan Society of Applied Electromagnetics and Mechanics, Vol.14, pp.387-388

S. Yamamura, K. Ohnishi, E. Masada, 1979 "Theory of Control System of Electromagnetically Levitated Bogie-truck." The Institute of Electrical Engineers of Japan, Vol.99 No.11, pp.752-759